

Automated Diagnosis of Glaucoma using Haralick Texture Features

Simonthomas.S¹, Thulasi.N²

¹(Department of Computer Science & engineering, Anna University, India)

²(Department of Computer Science & engineering, Anna University, India)

Abstract : Glaucoma is the second leading cause of blindness worldwide. It is a disease in which fluid pressure in the eye increases continuously, damaging the optic nerve and causing vision loss. Computational decision support systems for the early detection of glaucoma can help prevent this complication. The retinal optic nerve fibre layer can be assessed using optical coherence tomography, scanning laser polarimetry, and Heidelberg retina tomography scanning methods. In this paper, we present a novel method for glaucoma detection using an Haralick Texture Features from digital fundus images. K Nearest Neighbors (KNN) classifiers are used to perform supervised classification. Our results demonstrate that the Haralick Texture Features has Database and classification parts, in Database the image has been loaded and Gray Level Co-occurrence Matrix (GLCM) and thirteen haralick features are combined to extract the image features, performs better than the other classifiers and correctly identifies the glaucoma images with an accuracy of more than 98%. The impact of training and testing is also studied to improve results. Our proposed novel features are clinically significant and can be used to detect glaucoma accurately.

Keywords: Glaucoma, Haralick Texture features, KNN Classifiers, Feature Extraction

I. INTRODUCTION

This GLAUCOMA is the second leading cause of peripheral blindness worldwide and results in the neurodegeneration of the optic nerve. As the revitalization of the degenerated optic nerve fibers is not viable medically, glaucoma often goes undetected in its patients until later stages. The prevalent model estimates that approximately 11.1million patients worldwide will suffer from glaucoma induced bilateral blindness in 2020. Furthermore, in countries, like India, it is estimated that approximately 11.2 million people over the age of 40 suffer from glaucoma. It is believed that these numbers can be curtailed with effective detection and treatment options. In light of the diagnostic challenge at hand, recent advances in biomedical imaging offer effective quantitative imaging alternatives for the detection and management of glaucoma. Several imaging modalities and their enhancements, including optical coherence tomography and multifocal electroretinograph (mfERG), are prominent techniques employed to quantitatively analyze structural and functional abnormalities in the eye both to observe variability and to quantify the progression of the disease objectively.

Automated clinical decision support systems (CDSSs) in ophthalmology, such as CASNET/glaucoma, are designed to create effective decision support systems for the identification of disease pathology in human eyes. These CDSSs have used glaucoma as a predominant case study for decades. Such CDSSs are based on retinal image analysis techniques that are used to extract structural, contextual, or textural features from retinal images to effectively distinguish between normal and diseased samples. Retinal image analysis techniques rely on computational techniques to make qualitative assessments of the eye more reproducible and objective. The goal of using such methods is to reduce the variability that may arise between different clinicians tracking the progression of structural characteristics in the eye. In CDSS, features extracted from the images are categorized as either structural features or texture features. Commonly categorized structural features include disk area, disk diameter, rim area, cup area, cup diameter, cup-to-disk ratio, and topological features extracted from the image. Proper orthogonal decomposition (POD) is an example of a technique that uses structural features to identify glaucomatous progression. In POD, pixel-level information is used to gauge significant changes across samples that are location or region specific. The measurement of texture features, on the other hand, is roughly defined as the spatial variation of pixel intensity (gray-scale values) across the image. Textural features are, thus, not bound to specific locations on the image. Several feature extraction techniques, including spectral techniques, are available to mine texture features.

a general procedure for extracting textural properties of blocks of image data. These features are calculated in the spatial domain, and the statistical nature of texture is taken into account in our procedure, which is based on the assumption that the texture information in an image I is contained in the overall or "average" spatial relationship which the gray tones in the image have to one another. We compute a set of graytone spatial-dependence probability-distribution matrices for a given image block and suggest a set of 14 textural features which can be extracted from each of these matrices. These features contain information about

such image textural characteristics as homogeneity, gray-tone linear dependencies (linear structure), contrast, number and nature of boundaries present, and the complexity of the image. It is important to note that the number of operations required to compute any one of these features is proportional to the number of resolution cells in the image block. It is for this reason that we call these features quickly computable.

Our initial perspective of texture and tone is based on the concept that texture and tone bear an inextricable relationship to one another. Tone and texture are always present in an image, although one property can dominate the other at times. The basic intuitively perceived relationships between tone and texture are the following. When a small-area patch of an image has little variation-i.e., little variation of features of discrete gray tone-the dominant property of that area is tone. When a small-area patch has a wide variation of features of discrete gray tone, the dominant property of that area is texture. Crucial to this distinction are the size of the small-area patch, the relative sizes of the discrete features, and the number of distinguishable discrete features.

As the number of distinguishable tonal discrete features decreases, the tonal properties will predominate. In fact, when the small-area patch is only the size of one resolution cell, so that there is only one discrete feature, the only property present is tone. As the number of distinguishable features of discrete gray tone increases within the small-area patch, the texture property will dominate. One important property of tone-texture is the spatial pattern of the resolution cells composing each discrete tonal feature. When there is no spatial pattern and the gray-tone variation between features is wide, a fine texture results. As the spatial pattern becomes more definite and involves more and more resolution cells, a coarser texture results. An excellent set of photographs of different types of texture may be found.

The preceding description of texture is, of course, a gross simplification and idealization of what actually occurs. Discrete tonal features are really quite fuzzy in that they do not necessarily stand out as entities by themselves. Therefore the texture analysis we suggest is concerned with more general or macroscopic concepts than discrete tonal features. The procedure we suggest for obtaining the textural features of an image is based on the assumption that the texture information on an image I is contained in the overall or "average" spatial relationship which the gray tones in the image I have to one another. More specifically, we shall assume that this texture information is adequately specified by a set of gray-tone spatial-dependence matrices which are computed for various angular relationships and distances between neighboring resolution cell pairs on the image. All of our textural features are derived from these angular nearest-neighbor gray-tone spatial-dependence matrices.. (10)

II. DATASET

The digital retinal images were collected from the Kasturba Medical College, Manipal, India (<http://www.manipal.edu>). The doctors in the ophthalmology department of the hospital manually curated the images based on the quality and usability of samples. The ethics committee, consisting of senior doctors, approved the use of the images for this research.

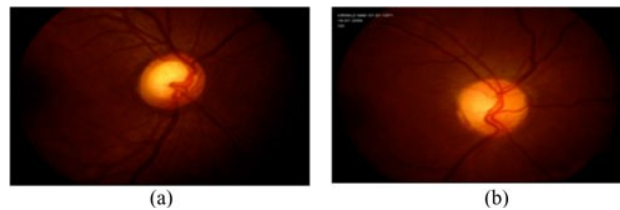


Fig. 1. Typical fundus images. (a).Normal. (b).Glaucoma

All the images were taken with a resolution of 560×720 pixels and stored in lossless JPEG format [10]. The dataset contains 60 fundus images: 30 normal and 30 open angle glaucomatous images from 20 to 70 year-old subjects. The fundus camera, a microscope, and a light source were used to acquire the retinal images to diagnose diseases. Fig. 1(a) and (b) presents typical normal and glaucoma fundus images, respectively.

III. METHODOLOGY

A set of descriptive features that are fundamentally different from the Zernike moments, the texture features described by Haralick, were investigated next. These features were selected because they can be made invariant to translations and rotations, and because they describe more intuitive aspects of the images (e.g. coarse versus smooth, directionality of the pattern, image complexity, etc.) using statistics of the gray-level co-occurrence matrix for each image. An image processing techniques to diagnose the glaucoma based on the Haralick evaluation of preprocessed fundus images. These algorithms are tested on publicly available fundus images and the results are compared. The accuracy of these algorithms is evaluated by sensitivity and specificity. The sensitivity and specificity for these algorithms are found to be very favorable.

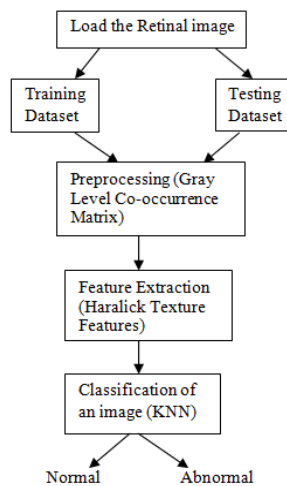


Fig 2:Proposed glaucoma detection System

This paper focused on the description of a system based on image processing and classification techniques for the estimation of quantitative parameters to classify fundus images into two classes: glaucoma patients and normal patients.

a. Gray Level Co-occurrence Matrix:

A GLCM $P[i,j]$ is defined by specifying displacement vector $d=(dx,dy)$. Counting all pairs of pixels separated by d , having gray levels i and j . GLCM Measures are, Entropy-Randomness of gray level distribution, Energy-uniformity of gray level in a region, Contrast-Measure of difference between gray levels and Homogeneity-Measure of similarity of texture. Suppose an image to be analyzed is rectangular and has N_x resolution cells in the horizontal direction and N_y resolution cells in the vertical direction. Suppose that the gray tone appearing in each resolution cell is quantized to N_g levels. Let $L_x = \{1,2, \dots, N_x\}$ be the horizontal spatial domain, $L_y = \{1,2, \dots, N_y\}$ be the vertical spatial domain, and $G = \{1,2, \dots, N_g\}$ be the set of N_g quantized gray tones. The set $L_y \times L_x$ is the set of resolution cells of the image ordered by their row-column designations. The image I can be represented as a function which assigns some gray tone in G to each resolution cell or pair of coordinates in $L_y \times L_x$; $I: L_y \times L_x \rightarrow G$.

An essential component of our conceptual framework of texture is a measure, or more precisely, four closely related measures from which all of our texture features are derived. These measures are arrays termed angular nearest-neighbor gray-tone spatial-dependence matrices, and to describe these arrays we must emphasize our notion of adjacent or nearest-neighbor resolution cells themselves. We consider a resolution cell-excluding those on the periphery of an image, etc.-to have eight nearest-neighbor resolution.

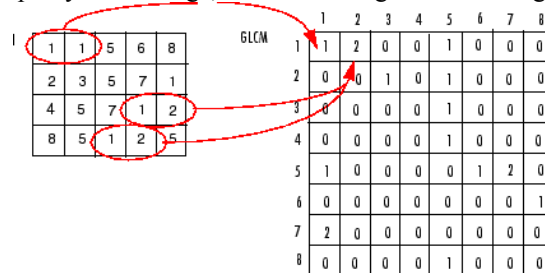


Fig 3: graycomatrix continues this processing to fill in all the values in the GLCM

Syntax for Calculating GLCM,

```

gcm = graycomatrix(I)
gcmS = graycomatrix(I, param1, val1, param2, val2,...)
[gcm, SI] = graycomatrix(...)
  
```

`gcm = graycomatrix(I)` creates a gray-level co-occurrence matrix (GLCM) from image I . `graycomatrix` creates the GLCM by calculating how often a pixel with gray-level (grayscale intensity) value i occurs horizontally adjacent to a pixel with the value j . (You can specify other pixel spatial relationships using the 'Offsets' parameter -- see Parameters.) Each element (i,j) in `gcm` specifies the number of times that the pixel with value i occurred horizontally adjacent to a pixel with value j . `graycomatrix` calculates the GLCM from a scaled version of the image. By default, if I is a binary image, `graycomatrix` scales the image to two gray-levels.

If I is an intensity image, graycomatrix scales the image to eight gray-levels. we can specify the number of gray-levels graycomatrix uses to scale the image by using the 'NumLevels' parameter, and the way that graycomatrix scales the values using the 'GrayLimits' parameter. graycomatrix calculates several values in the GLCM of the 4-by-5 image I. Element (1,1) in the GLCM contains the value 1 because there is only one instance in the image where two, horizontally adjacent pixels have the values 1 and 1. Element (1,2) in the GLCM contains the value 2 because there are two instances in the image where two, horizontally adjacent pixels have the values 1 and 2. graycomatrix continues this processing to fill in all the values in the GLCM.

b. Haralick Texture Features:

Haralick's texture features were calculated using the kharalick() function. The basis for these features is the gray-level co-occurrence matrix (**G** in Equation 1). This matrix is square with dimension N_g , where N_g is the number of gray levels in the image. Element $[i,j]$ of the matrix is generated by counting the number of times a pixel with value i is adjacent to a pixel with value j and then dividing the entire matrix by the total number of such comparisons made. Each entry is therefore considered to be the probability that a pixel with value i will be found adjacent to a pixel of value j .

$$G = \begin{bmatrix} p(1,1) & p(1,2) & \dots & p(1, N_g) \\ p(2,1) & p(2,2) & \dots & p(2, N_g) \\ \vdots & \vdots & \ddots & \vdots \\ p(N_g, 1) & p(N_g, 2) & \dots & p(N_g, N_g) \end{bmatrix} \dots\dots\dots(1)$$

Since adjacency can be defined to occur in each of four directions in a 2D, square pixel image (horizontal, vertical, left and right diagonals-Fig:4), four such matrices can be calculated.

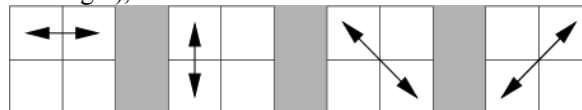


Fig 4: Four directions of adjacency as defined for calculation of the Haralick texture features.

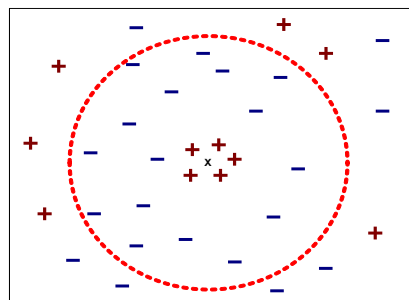
The Haralick statistics are calculated for co-occurrence matrices generated using each of these directions of adjacency.

c. KNN Classifier:

A nearest-neighbor classification object, where both distance metric ("nearest") and number of neighbors can be altered. The object classifies new observations using the predict method. The object contains the data used for training, so can compute resubstitution predictions. The key issues involved in training this model includes setting 1. the variable K, Validation techniques (ex. Cross validation) 2.the type of distant metric, Euclidean measure is,

$$Dist(X,Y)=\sqrt{\sum_{i=1}^D(X_i - Y_i)^2}$$

k NN-find the k closest training points (small $kx_i - x_0k$ according to some metric) 1.predicted class: majority vote 2.predicted value: average weighted by inverse distance.



Calculate distances of all training vectors to test vector. Pick k closest vectors. Calculate average/majority.

IV. FEATURE EXTRACTION

Haralick Texture Features which can be extracted from each of the gray-tone spatial-dependence matrices. The following equations defines these feature,

Notations:

- $P(i,j)$ (i,j)th entry in a normalization gray-tone spatial dependence matrix, $=p(i,j)/R$
- $P_x(i)$ i th entry in the marginal probability matrix obtained by summing the rows of $p(i,j)$.

N_g Number of distinct gray levels in the quantized image
 \sum_i and \sum_j $\sum_{i=1}^{N_g}$ and $\sum_{j=1}^{N_g}$, respectively
 $p_y(j) = \sum_{i=1}^{N_g} p(i, j)$
 $p_{x+y}(k) = \sum_{i=1}^{N_g} \sum_{j=1}^{N_g} p(i, j)$, $k = 2, 3, \dots, 2N_g$
 $p_{x-y}(k) = \sum_{i=1}^{N_g} \sum_{j=1}^{N_g} p(i, j)$, $k = 0, 1, \dots, N_g - 1$

The Haralick Texture Features are,

1. Angular Second Moment:

$$f_1 = \sum_i \sum_j \{p(i, j)\}^2$$

2. Contrast:

$$f_2 = \sum_{n=0}^{N_g-1} n^2 \left\{ \sum_{i=1}^{N_g} \sum_{j=1}^{N_g} p(i, j) \right\}$$

3. Correlation:

$$f_3 = \frac{\sum_i \sum_j (ij) p(i, j) - \mu_x \mu_y}{\sigma_x \sigma_y}$$

where, μ_x , μ_y , σ_x and σ_y are the mean and standard deviations of p_x and p_y .

4. Sum of squares: Variance

$$f_4 = \sum_i \sum_j (i - \mu)^2 p(i, j)$$

5. Inverse Difference Moment:

$$f_5 = \sum_i \sum_j \frac{1}{1+(i-j)^2} p(i, j)$$

6. Sum Average:

$$f_6 = \sum_{i=2}^{2N_g} i p_{x+y}(i)$$

7. Sum Variance:

$$f_7 = \sum_{i=2}^{2N_g} (i - f_6)^2 p_{x+y}(i)$$

8. Sum Entropy:²

$$f_8 = - \sum_{i=2}^{2N_g} p_{x+y}(i) \log\{p_{x+y}(i)\}$$

9. Entropy:

$$f_9 = - \sum_i \sum_j p(i, j) \log(p(i, j))$$

10. Difference Variance:

$$f_{10} = \text{variance of } p_{x-y}$$

11. Difference Entropy:

$$f_{11} = - \sum_{i=0}^{N_g-1} p_{x-y}(i) \log\{p_{x-y}(i)\}$$

12,13. Information of Correlation:

$$f_{12} = \frac{H_{XY} - H_{XY1}}{\max\{H_X, H_Y\}}$$

$$f_{13} = (1 - \exp[-2.0(H_{XY2} - H_{XY})])^{1/2}$$

$$H_{XY} = - \sum_i \sum_j p(i, j) \log(p(i, j))$$

Where H_X and H_Y are entropies of p_x and p_y , and

$$H_{XY1} = - \sum_i \sum_j p(i, j) \log\{p_x(i)p_y(j)\}$$

$$H_{XY2} = \sum_i \sum_j p_x(i)p_y(j) \log\{p_x(i)p_y(j)\}$$

14. Maximal Correlation Coefficient:

$$f_{14} = (\text{Second largest eigenvalues of } Q)^{1/2}$$

Where,

$$Q(i,j) = \sum_k \frac{p(i,k)p(j,k)}{p_x(i)p_y(k)}$$

These measures of correlation have some desirable properties which are not brought out in the rectangular correlation measures f_3 . The text for Chosen distance d we have four angular gray-tone spatial-dependency matrices. Hence we obtain a set of four values for each of preceding 14 measures. The mean and range of each of these 14 measures, averaged over the four values, comprise the set of 28 features which can be used as input to the classifier. In this set of 28 features some of the features are strongly correlated with each other. A feature-selection procedure may be applied to select a subset or linear combinations of the 28 features.

V. CONCLUSION

In this paper, we developed an automatic glaucoma diagnosis system using haralick texture features extracted from fundus images for diagnosis. We found that the haralick texture features were significant, i.e., the features has been extracted from the glcm and the pixel values has been calculates based on the haralick co-occurrence matrix values. Training and testing datasets are used to classify the KNN classifier to finding the pixel values to each and every matrix values, and finding the normal and abnormal(glaucoma affected) images with the classification accuracy of above 98%. Our technique is of clinical significance, as the accuracy obtained is comparable to the accuracies achieved so far in the existing systems. The classification accuracy can be further improved by increasing the number of diverse training images, choosing better features and better classifiers and using controlled environmental lighting conditions during image acquisition. using more diverse digital fundus images from normal and glaucoma subjects can further enhance the percentage of correct diagnosis. We can conclude that the energy obtained from the detailed coefficients can be used to distinguish between normal and glaucomatous images with very high accuracy.

VI. REFERENCES

Journal Papers:

- [1] R. Haralick, K. Shanmugam, and I. Dinstein, (1973) "Textural Features for Image Classification", IEEE Trans. on Systems, Man and Cybernetics, SMC-3(6):610-621
- [2] Sumeet Dua, *Senior Member, IEEE*, U. Rajendra Acharya, Pradeep Chowriappa "Wavelet-Based Energy Features for Glaucomatous Image Classification" VOL. 16, NO. 1, JANUARY 2012
- [3] U.Rajendra Acharya, Sumeet Due, Xian Du, and Vinitha Sree S "Automated Diagnosis of Glaucoma Using Textural and Higher Order Spectra Features"

Books:

- [4] R. C. Gonzales, R. E. Woods, and S. L. Eddins. Digital Image Processing Using MATLAB.

Chapters in Books:

- [5] J. M. Miquel-Jimenez *et al.*, "Glaucoma detection by wavelet-based analysis of the global flash multifocal electroretinogram," *Med. Eng. Phys.*, vol. 32, pp. 617-622, 2010
- [6] Bino Sebastian V, A. Unnikrishnan and Kannan Balakrishnan "grey level co-occurrence matrices: generalisation and some new features" (IJCSEIT), Vol.2, No.2, April 2012
- [7] F. I. Alam, R. U. Faruqui, (2011) "Optimized Calculations of Haralick Texture Features", European Journal of Scientific Research, Vol. 50 No. 4, pp. 543-553

Theses:

- [8] Celina Rani George "Glaucomatous Image Classification Using Wavelet Based Energy Signatures And Neural Networks" (IJERT) ISSN: 2278-0181 Vol. 2 Issue 3, March - 2013
- [9] Miguel-Jiménez J M, Blanco R, "Glaucoma detection by wavelet-based analysis of the global flash multifocal electroretinogram," *Med. Eng. Phys.*, vol. 32, pp. 617-622, 2010.

Proceedings Papers:

- [10] P. C. Chen and T. Pavlidis, "Segmentation of texture using correlation," *IEEE Trans. Pattern Anal. Machine Intell.*, vol. PAMI-5, pp. 64-69, Jan. 1983.
- [11] Tou, J. Y., Tay, Y. H., & Lau, P. Y. (2009). Recent Trends in Texture Classification: A Review. Proceedings Symposium on Progress, in Information and Communication Technology 2009 (SPICT 2009), Kuala Lumpur, pp. 63-68.
- [12] A. Laine and J. Fan, "Texture classification by wavelet packet signatures," *IEEE Trans. Pattern Recognit. Machine Intell.*, vol. 15, pp. 1186-1191,